

Recent Advances in Potentiometric Scanning Electrochemical Microscopy

author:
András Kiss

supervisor:
prof. Géza Nagy

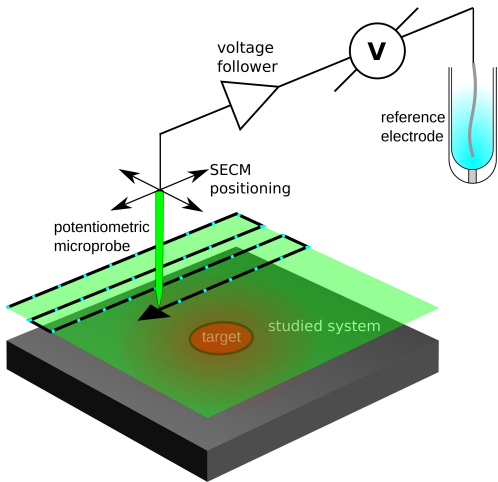
Department of General and Physical Chemistry
University of Pécs, Hungary



April 18, 2017

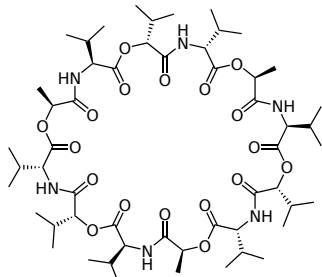
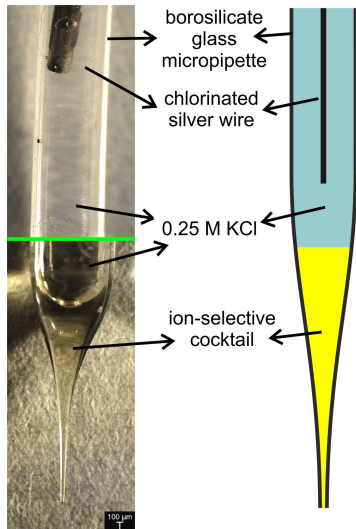
Potentiometric Scanning Electrochemical Microscopy

A Scanning Probe Microscopic technique



Ion-selective micropipettes

As SECM probes



Valinomycin

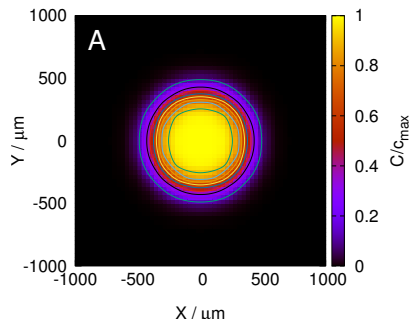
$$E = E^\theta + \frac{RT}{z_i F} \ln \left[a_i + \sum_j \left(k_{ij} a_j^{z_i/z_j} \right) \right]$$

Nikolsky-equation

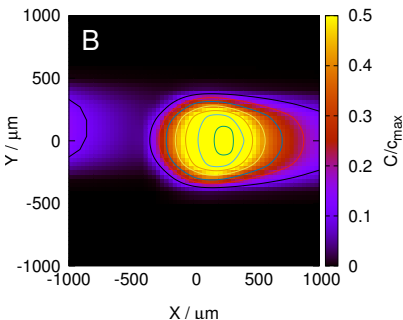
The problem with potentiometric SECM

Distortion at high scan rate

Slow

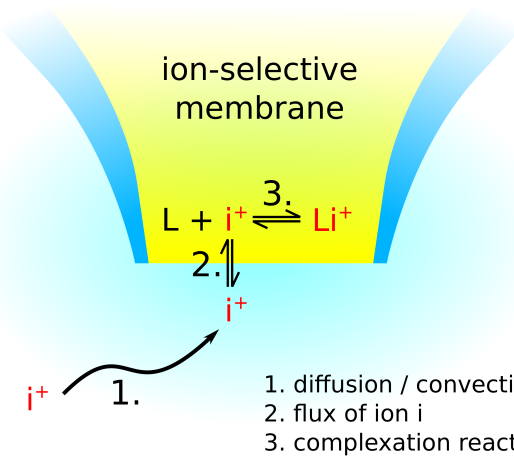


Fast



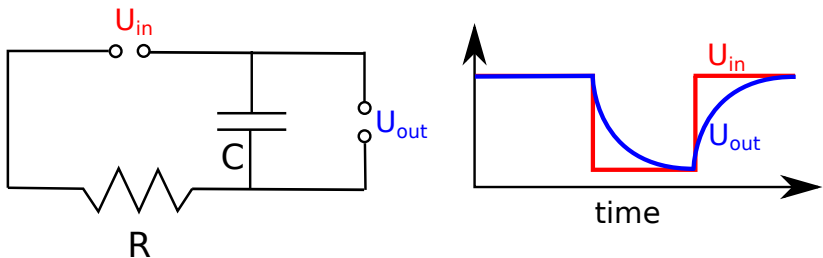
Why is the image distorted?

Possible contributors to the lag



Why is the image distorted?

The RC time constant



The time that is required to charge the capacitor by $\approx 63\%$ ($1 - 1/e$).

$$\tau = R \cdot C$$

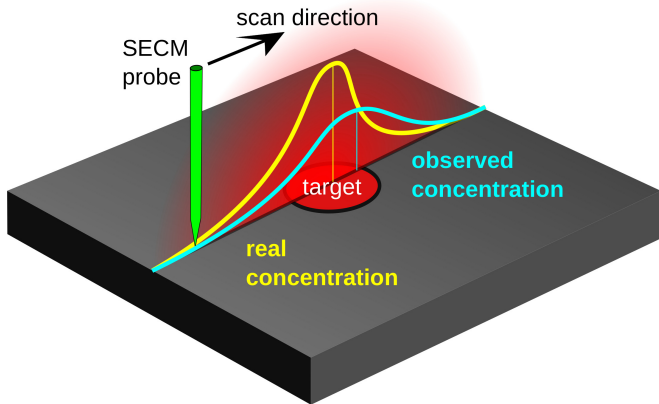
$$R = 5 \text{ G}\Omega$$

$$C = 500 \text{ pF}$$

$$\tau = 2.5 \text{ s}$$

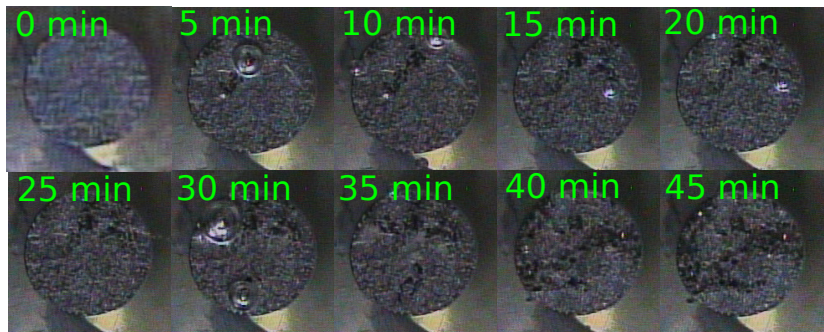
Distortion of potentiometric imaging

In the case of a linescan



Why is it so important to complete the scan quickly?

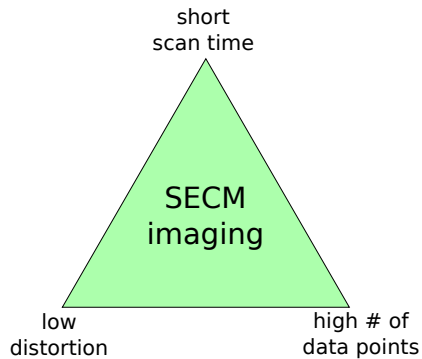
Example: corrosion of a magnesium alloy



Corrosion of the AZ63 magnesium-aluminium-zinc alloy.

Trade-off triangle of potentiometric SECM

Compromise between the three desired competing properties

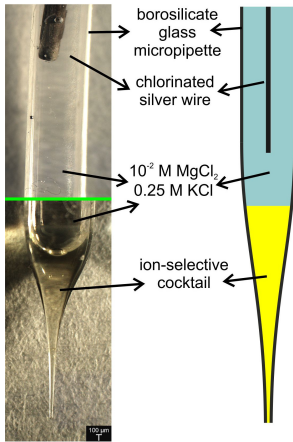


Solution #1: Solid contact micropipettes as SECM probes.

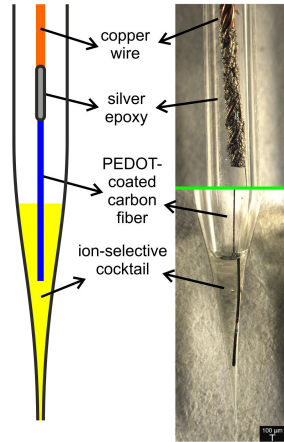
Liquid vs. solid contact micropipettes

Comparison of construction

Liquid contact

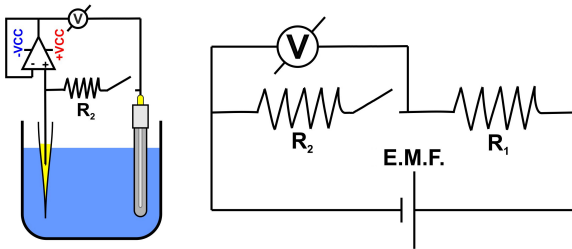


Solid contact



Comparison of the electrodes' resistance

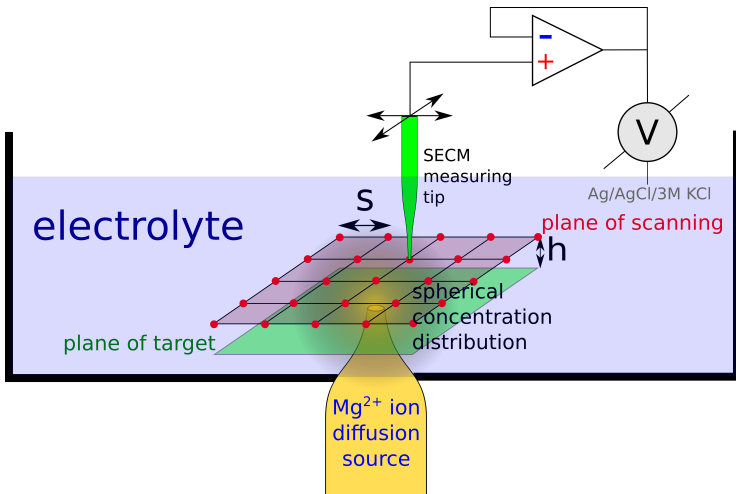
Voltage divider method and result



Type	$R_{ISME} / G\Omega$
Liquid contact	4.80
Solid contact	0.56

Comparison of the electrodes' performance

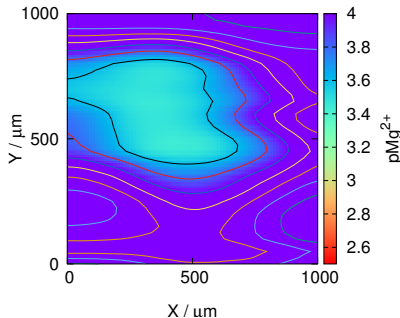
Experimental setup



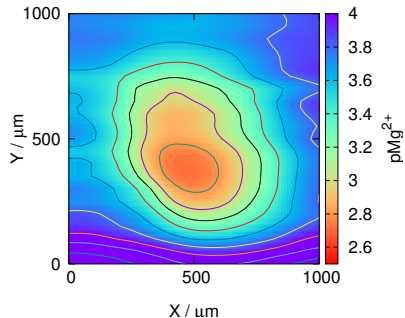
Comparison of the electrodes' performance

Results

Liquid contact

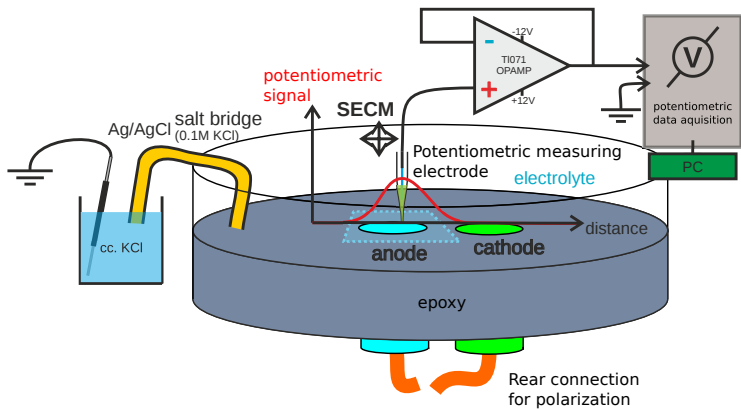


Solid contact



Application in corrosion science: galvanic corrosion of Mg

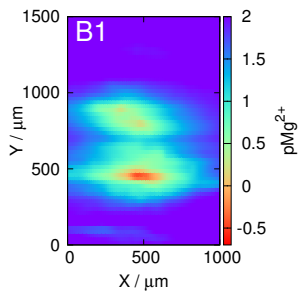
Experimental setup



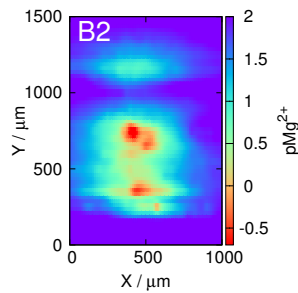
Application in corrosion science: galvanic corrosion of Mg

Results

Liquid contact



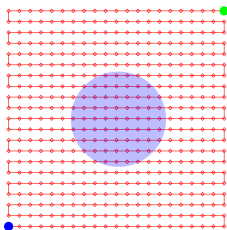
Solid contact



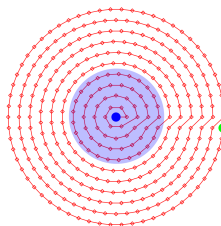
Solution #2: Optimizing scanning patterns and algorithms.

New SECM scanning patterns based on the polar-coordinate system

Cartesian coordinate
system based scanning
pattern



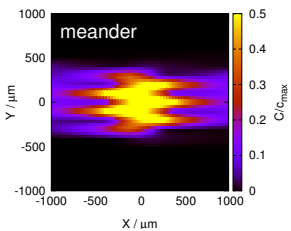
Polar coordinate
system based scanning
pattern



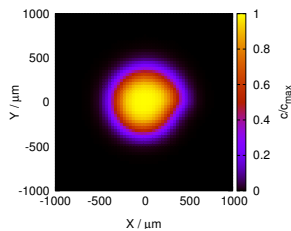
Simulated SECM scans

Using the Cartesian and the polar coordinate system based algorithms

Cartesian



polar

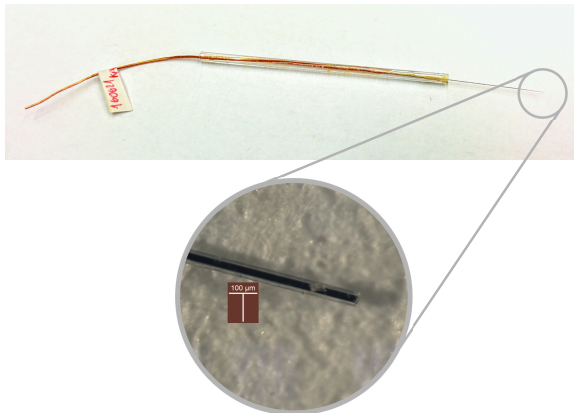


Comparison of the simulated scans

Algorithm	n	time (s)	mean squared error
Meander	441	440	2.75×10^{-2}
Fast comb	441	520	2.07×10^{-2}
Comb	441	881	2.75×10^{-2}
Web	110	109	9.63×10^{-3}
Arc	341	340	2.95×10^{-3}

Confirmation with experimental SECM scans

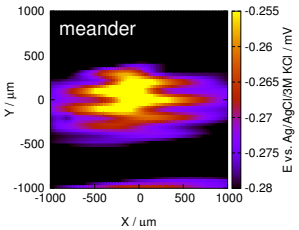
Antimony microelectrode as pH sensor



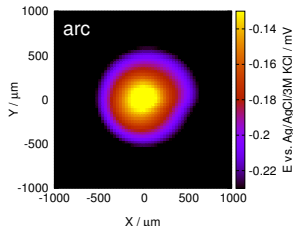
Confirmation with experimental SECM scans

Recorded using the antimony microelectrode

440 seconds



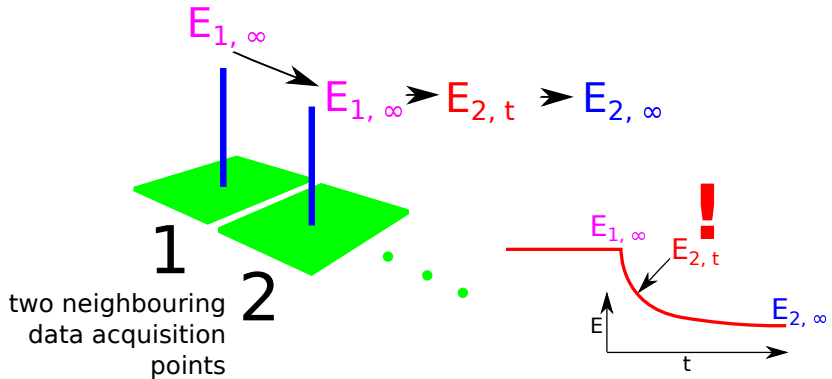
340 seconds



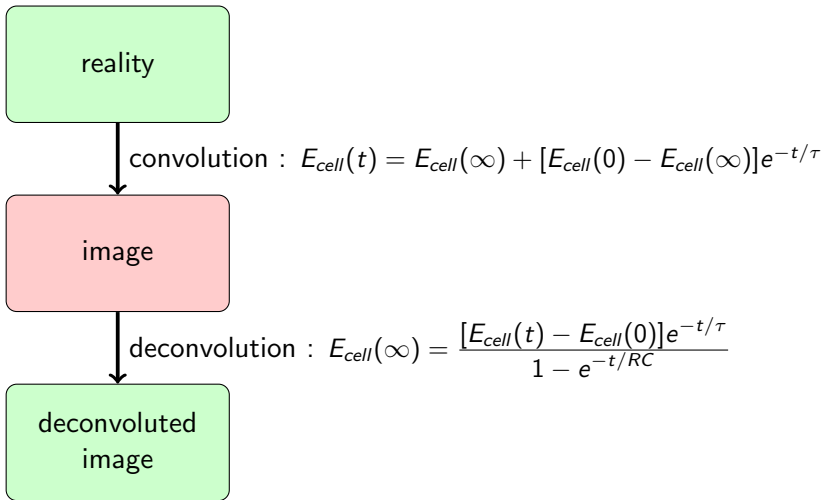
Scans are completed almost 2 times faster,
images have almost 10 times less distortion.

Solution #3: Signal processing.

The convolution function of the distortion

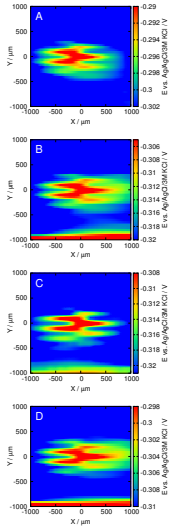


Convolution and deconvolution

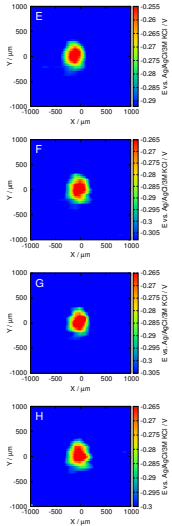


Deconvolution of potentiometric SECM images

Recorded using the antimony microelectrode following the meander algorithm

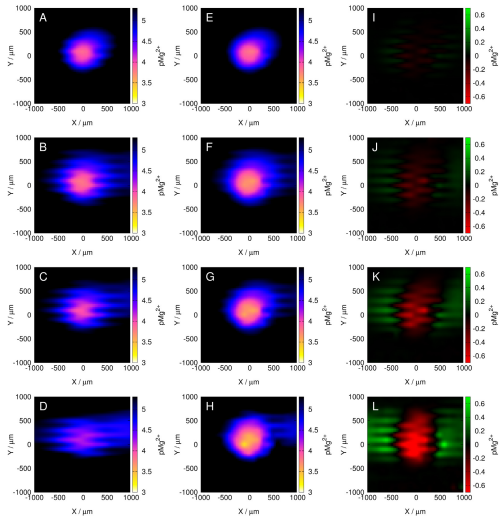


deconvolution
→



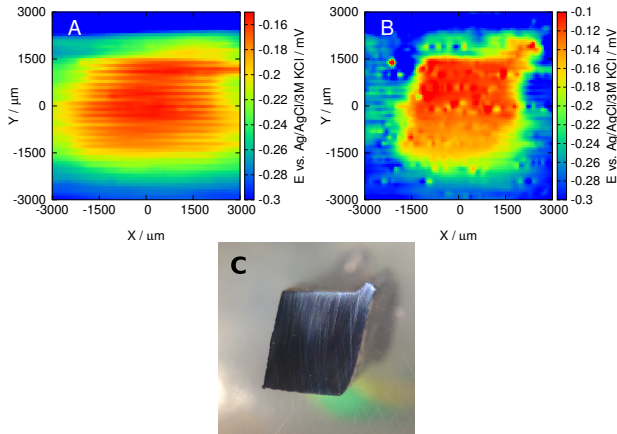
Deconvolution of potentiometric SECM images

Recorded using the magnesium ISME following the meander algorithm



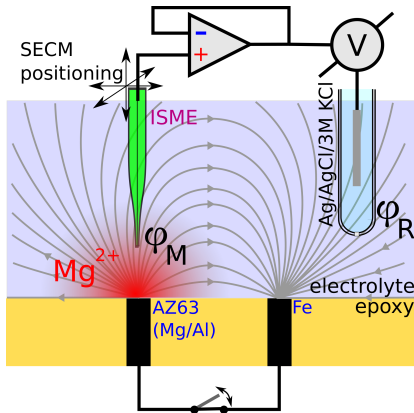
Practical example: corroding carbon steel sample

Scanned with an antimony microelectrode

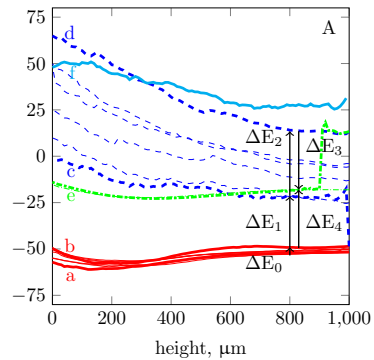
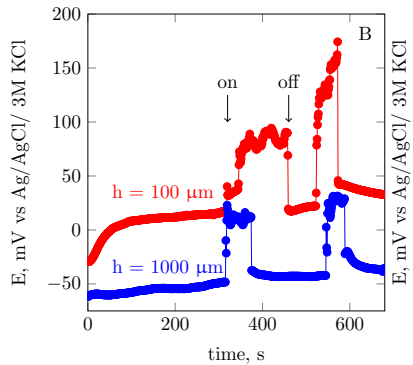


The effect of electric field on potentiometric SECM imaging.

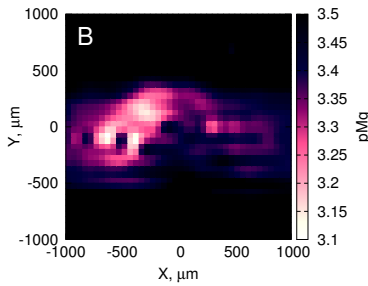
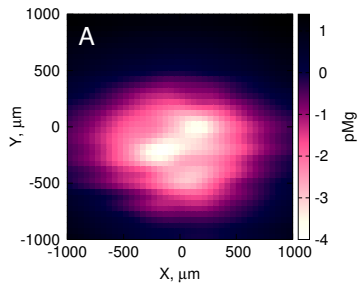
The electric field during galvanic corrosion



The effect of electric field on the measured potential



The effect of electric field on potentiometric SECM imaging



Conclusions

1. I've successfully shortened the response time of the potentiometric cell by using low resistance, solid-contact microelectrodes. I've compared them to conventional, liquid contact microelectrodes by basic characterization and model system study to prove the improved performance.
2. Taking advantage of the new solid-contact electrodes, I've studied the galvanic corrosion of magnesium and the AZ63 magnesium alloy by mapping the concentration of dissolving ions. I used the new solid contact ion selective microelectrodes as SECM probes. This allowed faster scan rates.

Conclusions

3. I've estimated the corrosion current based on the SECM measurements, and compared the result with that obtained with another, established method; the indirect measurement of corrosion current. After applying Faraday's Law of Electrolysis, the two results could be compared. They were very similar, suggesting the applicability of SECM in obtaining quantitative results.
4. I've designed new scanning patterns and algorithms, optimized to radially symmetric targets. I've proven that with these new patterns and algorithms, image distortion is lower compared to the conventional ones, by numerical simulations and experimental SECM scans.

Conclusions

5. I've shown that by using deconvolution, distortion can be significantly lowered in the potentiometric SECM images. To prove the validity of the technique, I've compared deconvoluted images to equilibrium images scanned at a rate which allowed to record equilibrium potentials.
6. I've used deconvolution to restore potentiometric SECM images about a corroding carbon steel sample. Evaluation of this data was possible, because scanning time *and* distortion was reduced at the same time.
7. I've shown the applicability of blind deconvolution. This method can be used on measurements where the convolution function cannot be determined.

Conclusions

8. I've proven that the electric field present in many studied systems – galvanically corroding ones in particular – affects the measured potential. The electric field has a direct influence on the measured potential, which is then a sum of this contribution and the Nernstian response associated with ion activity. This effect can cause serious errors in interpretations in the measurements. In this case, the error was almost four orders of magnitude. By taking this effect into account, a more accurate conclusion can be drawn.

Acknowledgements

List of publication

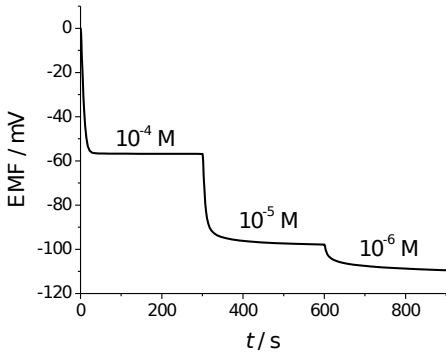


Figure 1. Nernst-Planck-Poisson simulation of the response of a potentiometric ion-selective sensor to decreasing primary ion activities. Relatively large activity of interfering ions is maintained ($a_J = 1\text{mM}$) to keep the whole cell R constant. Adhered layer thickness $100 \mu\text{m}$, $K_{IJ} = 10^{-3}$.